Supplementary Information

for

Trehalose-releasing nanogels reduce α-synuclein-induced Lewy body-like inclusions in primary mouse hippocampal neurons

Ali Maruf [1,2,3,†], Dmytro Gerasymchuk [3,†], Irena Hlushchuk [3], Safak Er [3,4], Małgorzata Milewska [1,2], Piotr Chmielarz [5], Andrii Domanskyi [6], Mikko Airavaara [3,*], Ilona Wandzik [1,2,*]

[1] Department of Organic Chemistry, Bioorganic Chemistry and Biotechnology, Faculty of Chemistry, Silesian University of Technology, Krzywoustego 4, 44-100 Gliwice, Poland

[2] Biotechnology Center, Silesian University of Technology, Krzywoustego 8, 44-100 Gliwice, Poland

[3] Division of Pharmacology and Pharmacotherapy, Drug Research Program, Faculty of Pharmacy, University of Helsinki, Viikinkaari 5E, 00790 Helsinki, Finland

[4] Department of Pharmacology, UCL School of Pharmacy, University College London, 29-39 Brunswick Square, London, WC1N 1AX, United Kingdom

[5] Department of Brain Biochemistry, Maj Institute of Pharmacology, Polish Academy of Sciences, Smętna 12, 31-343 Kraków, Poland

[6] Institute of Biotechnology, HiLIFE, University of Helsinki, Helsinki 00014, Finland

† The authors contribute equally

* Corresponding authors. E-mail addresses: mikko.airavaara@helsinki.fi (MA), ilona.wandzik@polsl.pl (IW)

Monomer feed compositions and physicochemical characteristics of nanogels

Table S1. Monomer feed compositions and physicochemical characteristics of nanogels

Nanogel	Trehalose monomer (mg, mmol)	Non-ionic monomer (mg, mmol)	Ionic monomer (mg, mmol)	Crosslinker (mg, mmol)	Yield (% w/w)	CTre (% w/w)	d_H (PDI) in DMEM (nm)	ζ-potential (mV)	Colloidal stability in serum-containing DMEM
TR	TreA (152.7, 0.385)	AM (35.3, 0.497)	AMPTMAC (17.6, 0.085)	MBAM (20.0, 0.130)	73	53.3	115 (0.21)	+30.2	Stable
TNR	TreA (152.7, 0.385)	DMAM (35.3, 0.385)	ATC (16.5, 0.085)	$PEG_{400}DA$ (67.0, 0.128)	76	47.0	145 (0.23)	+30.6	Stable

^{1}H NMR spectra of TreA, TR and TNR

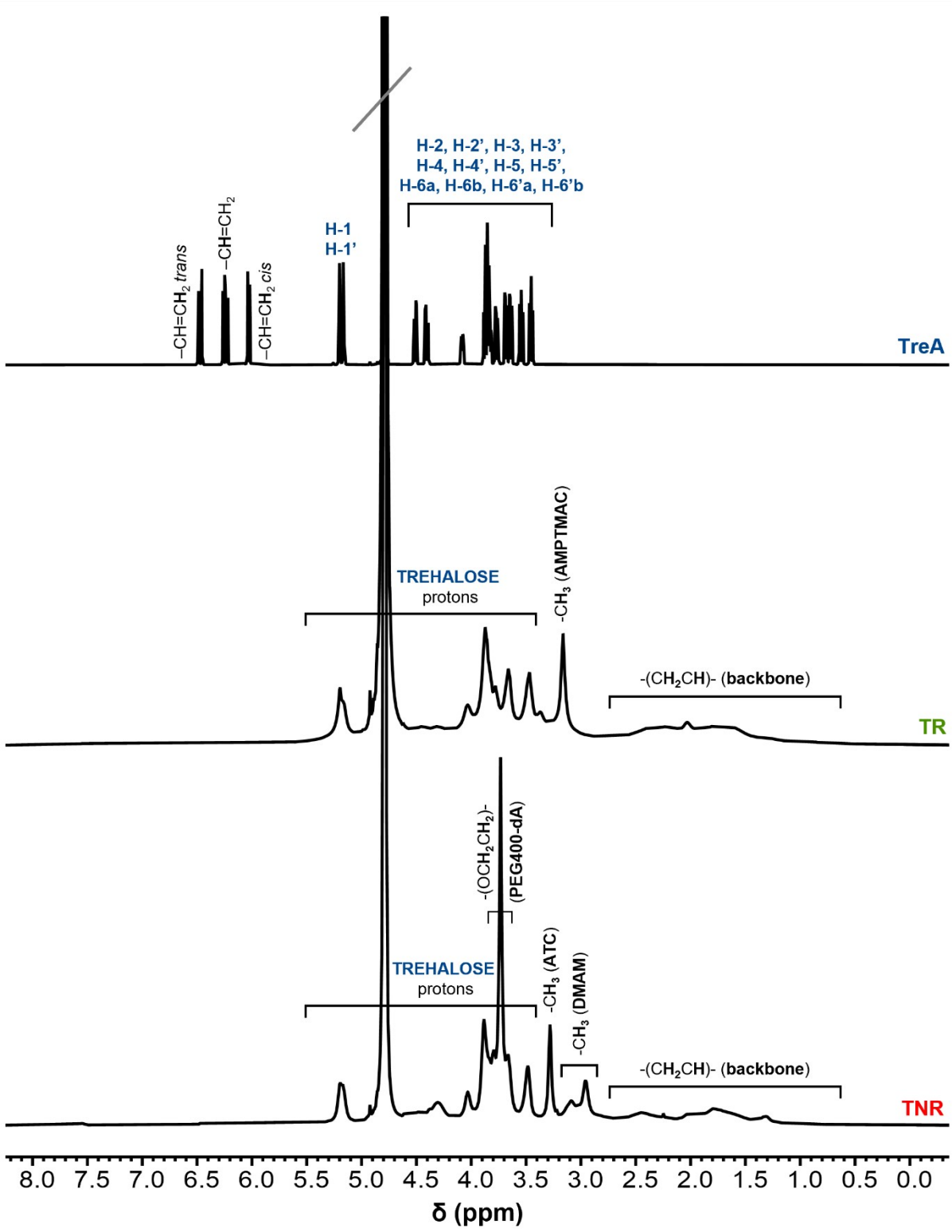

Figure S1. ^{1}H NMR spectra of TreA (top), TR (middle) and TNR (bottom). NMR spectra were recorded in deuterium oxide (Deutero GmbH) on Varian NMR instrument operating at 600 MHz. Chemical shifts are reported in ppm (δ) relative to the solvent residual signal.

Examples of LB analysis with CellProfiler and CellProfiler Analyst

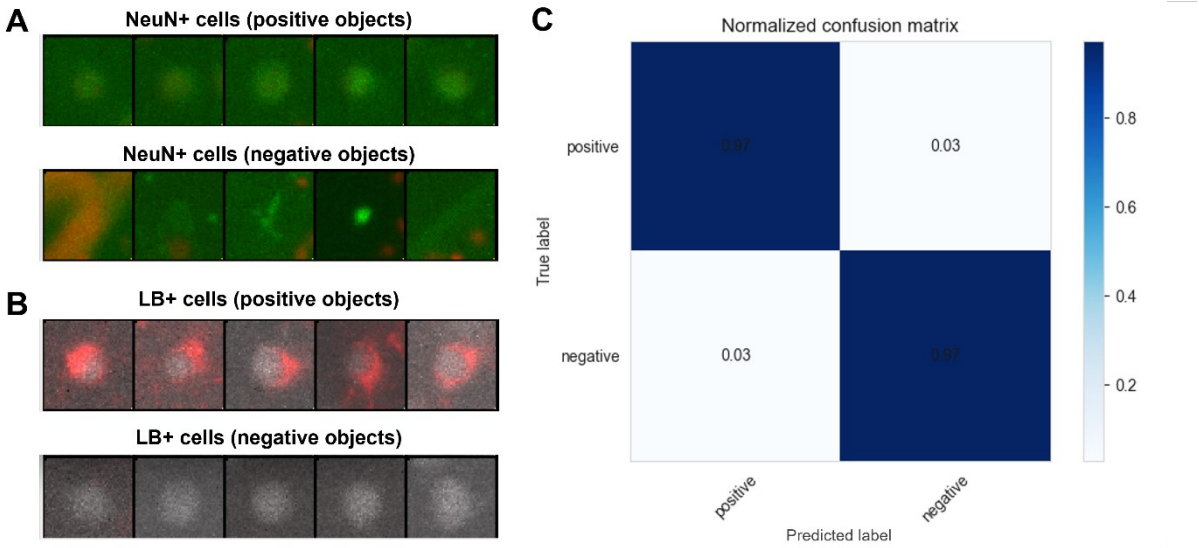

Figure S2. Analysis of LB-like inclusions with CellProfiler and CellProfiler Analyst software: examples of selected (A) NeuN+ cells and (B) LB+ NeuN+ cells both for positive objects and negative objects for training the software with minimum of 50 objects each object type for quantifying the total number of NeuN+ cells with or without LB-like inclusions per well. NeuN was visualized in green color in A, and grey color in B, while pS129Syn (α-synuclein) was visualized in red color in B. (C) Example of normalized confusion matrix obtained after training the software CellProfiler Analyst with the selected positive and negative objects: accepted values from 0.90 to 1.0 (navy blue) for the precision of calculation.

Pre-screening of starvation condition and lysosomal inhibitors (Baf, CA074, PepA, and SID) to be used in autophagy induction experiment in SH-SY5Y cells

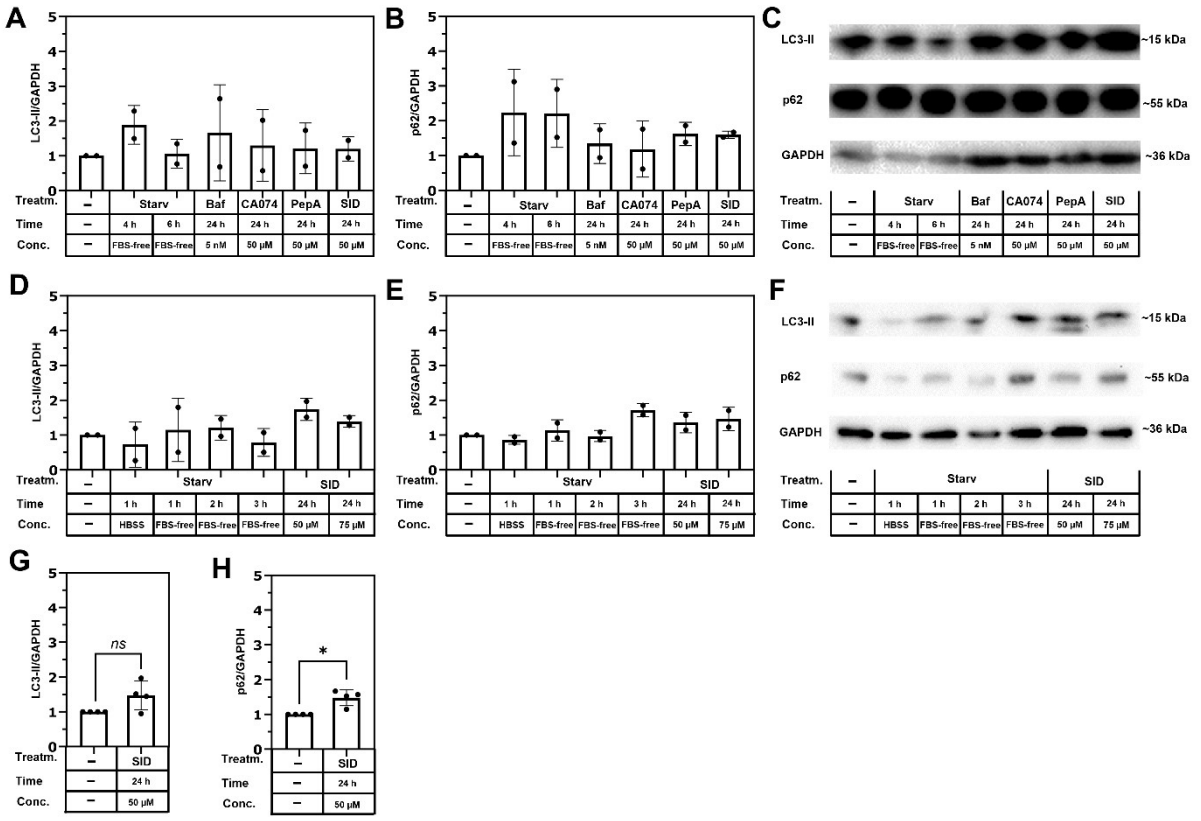

Figure S3. (A-F) Pre-screening of starvation condition and lysosomal inhibitors (Baf, CA074, PepA, and SID) to be used in autophagy induction experiment in SH-SY5Y cells, using LC3-II and p62 markers, assessed by Western blot analysis. Panels (C) and (F) show representative Western blot images of first and second pre-screening, respectively. (A, B) Quantification of LC3-II/GAPDH and p62/GAPDH ratios in the first pre-screening (control, 4 and 6 h of FBS-free starvation, CA074 50 μM, PepA 50 μM, and SID 50 μM). (D, E) Quantification of LC3-II/GAPDH and p62/GAPDH ratios in the second pre-screening (control, 1 h of HBSS starvation, 1, 2, and 3 h of FBS-free starvation, and SID 50 and 75 μM). (G, H) Quantification of LC3-II/GAPDH and p62/GAPDH ratios from the first and second pre-screening (combined) for SID 50 μM *vs* control. Data are presented as mean ± SD, from $n = 2$ independent experiments for A−F and 4 independent experiments for G and H. Statistical significance: *ns* = not significant, * $p < 0.05$; analyzed with paired *t*-test (G, H). Conclusion: Pre-screening of starvation condition and different lysosomal inhibitors was carried out to find suitable medium for conducting autophagy induction experiments with trehalose and nanogels. However, we could not find any suitable starvation condition, which should be marked with increasing LC3-II expression and decreasing p62 expression. Meanwhile, we found that SID 50 μM was an effective lysosomal inhibitor, in comparison to Baf, CA074, and PepA, which showed increasing both LC3-II and p62 expressions (G, H). These increased LC3-II and p62 levels were expected due to lysosomal blockade that prevent autophagosome/lysosome fusion and thus preventing cargo degradation leading to accumulation of autophagosome formation.

Therefore, the following autophagy induction experiments were conducted in normal medium *vs* SID 50 μM medium.

Cytotoxicity profiles of Tre, TR, and TNR in primary hippocampal neurons for 7 days tested with Presto Blue cell viability assay

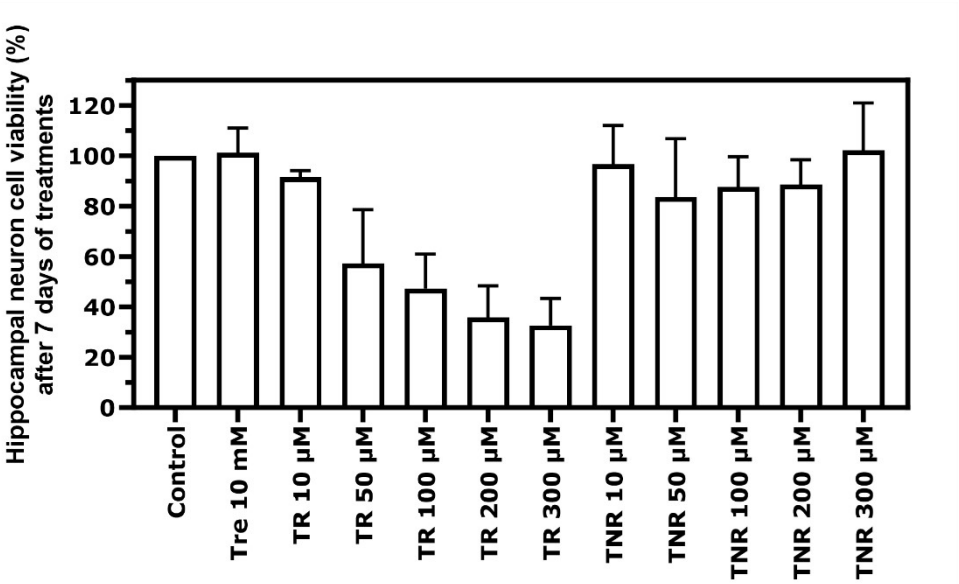

Figure S4. Cytotoxicity profiles of Tre (10 mM), TR (with equal trehalose concentrations of 10, 50, 100, 200 and 300 µM), and TNR (with equal trehalose concentrations of 10, 50, 100, 200 and 300 µM) in primary hippocampal neurons for 7 days of treatments. Data were normalized to control, n = 2 independent repeats with 3 technical repeats per treatment.

Cytotoxicity profiles of Tre, TR, and TNR in SH-SY5Y cells for 5 days tested with Presto Blue cell viability assay

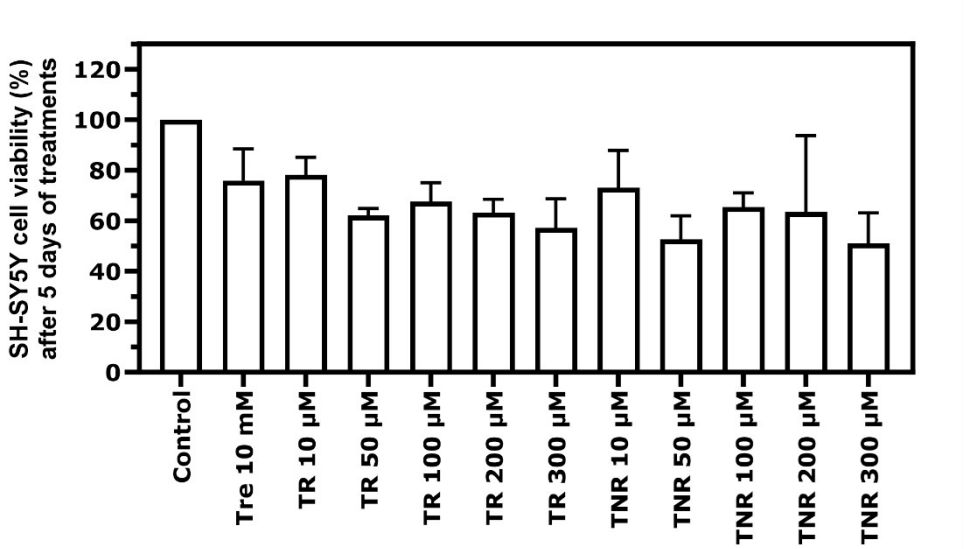

Figure S5. Cytotoxicity profiles of Tre (10 mM), TR (with equal trehalose concentrations of 10, 50, 100, 200 and 300 µM), and TNR (with equal trehalose concentrations of 10, 50, 100, 200 and 300 µM) in SH-SY5Y cells for 5 days of treatments. Data were normalized to control, n = 3 technical repeats.

Cytotoxicity profiles of different lysosomal inhibitors (Baf, CA074, PepA, and SID) for 24 h tested with Presto Blue cell viability assay

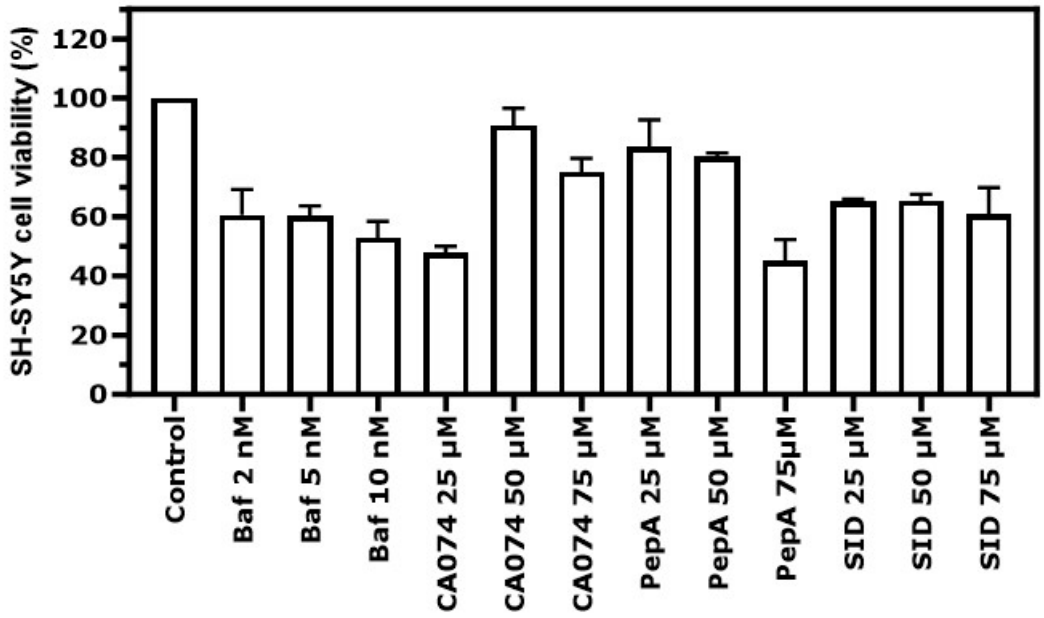

Figure S6. Cytotoxicity profiles of Baf (2, 5, and 5 nM), CA074 (25, 50, and 75 µM), PepA (25, 50, and 75 µM), and SID (25,50, and 75 µM) in SH-SY5Y cells for 24 h of treatments. Data were normalized to control, n = 3 technical repeats.

Quantification of LB-like inclusions in NeuN+ cells in the PBS treated groups (1-hour pre-treatment and 2, 4, and 24-hour post-treatments with compounds)

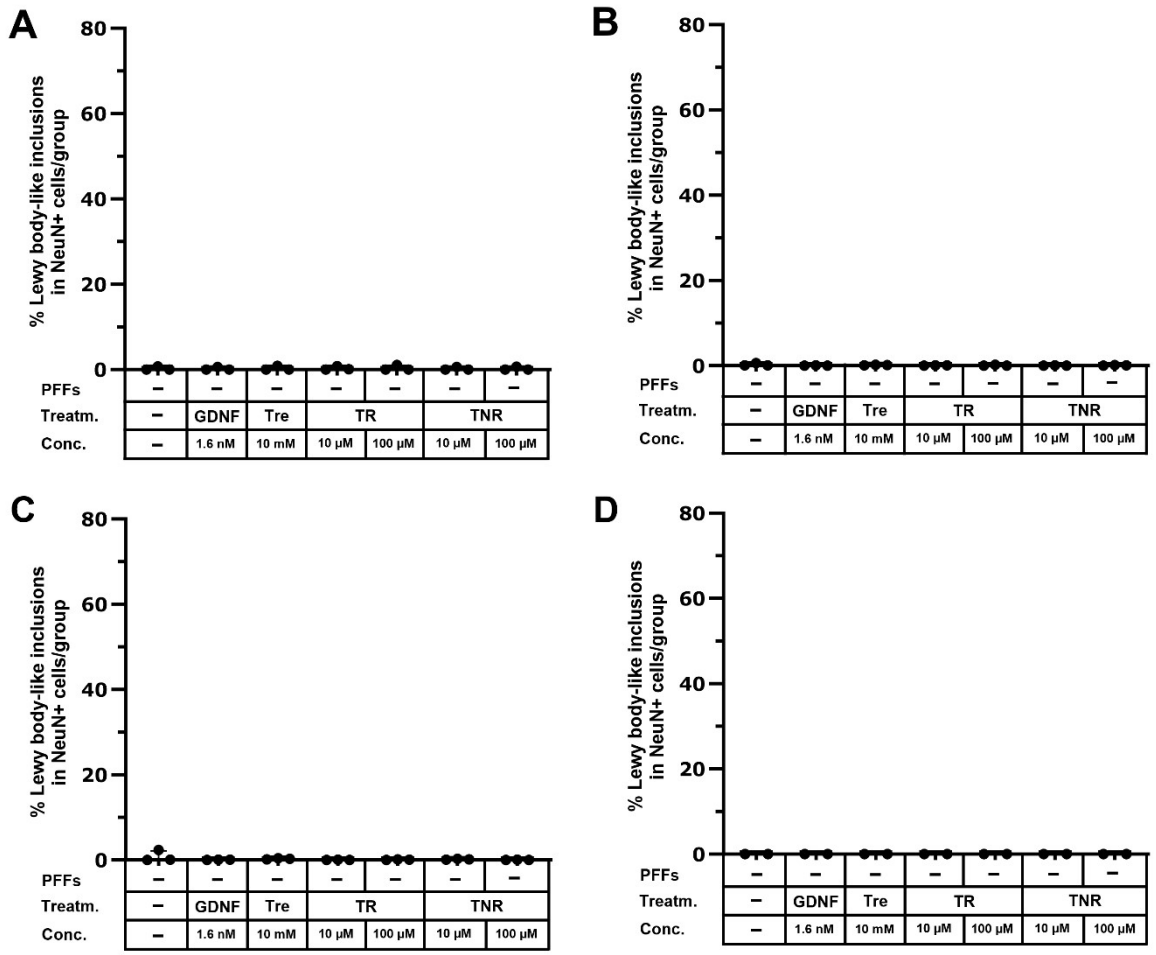

Figure S7. (A−D) Quantification of LB-like inclusions in NeuN+ cells, expressed as a percentage (%) in the PBS group for (A) 1-hour pre-treatment, (B) 2-hour post-treatment, (C) 4-hour post-treatment, and (D) 24-hour post-treatment. Data are presented as mean ± SD, from $n = 3$ independent experiments for A−C and $n = 2$ independent experiments for D.

Quantification of LB-like inclusions in NeuN+ cells treated with PFFs and test compounds (4-hour post-treatment)

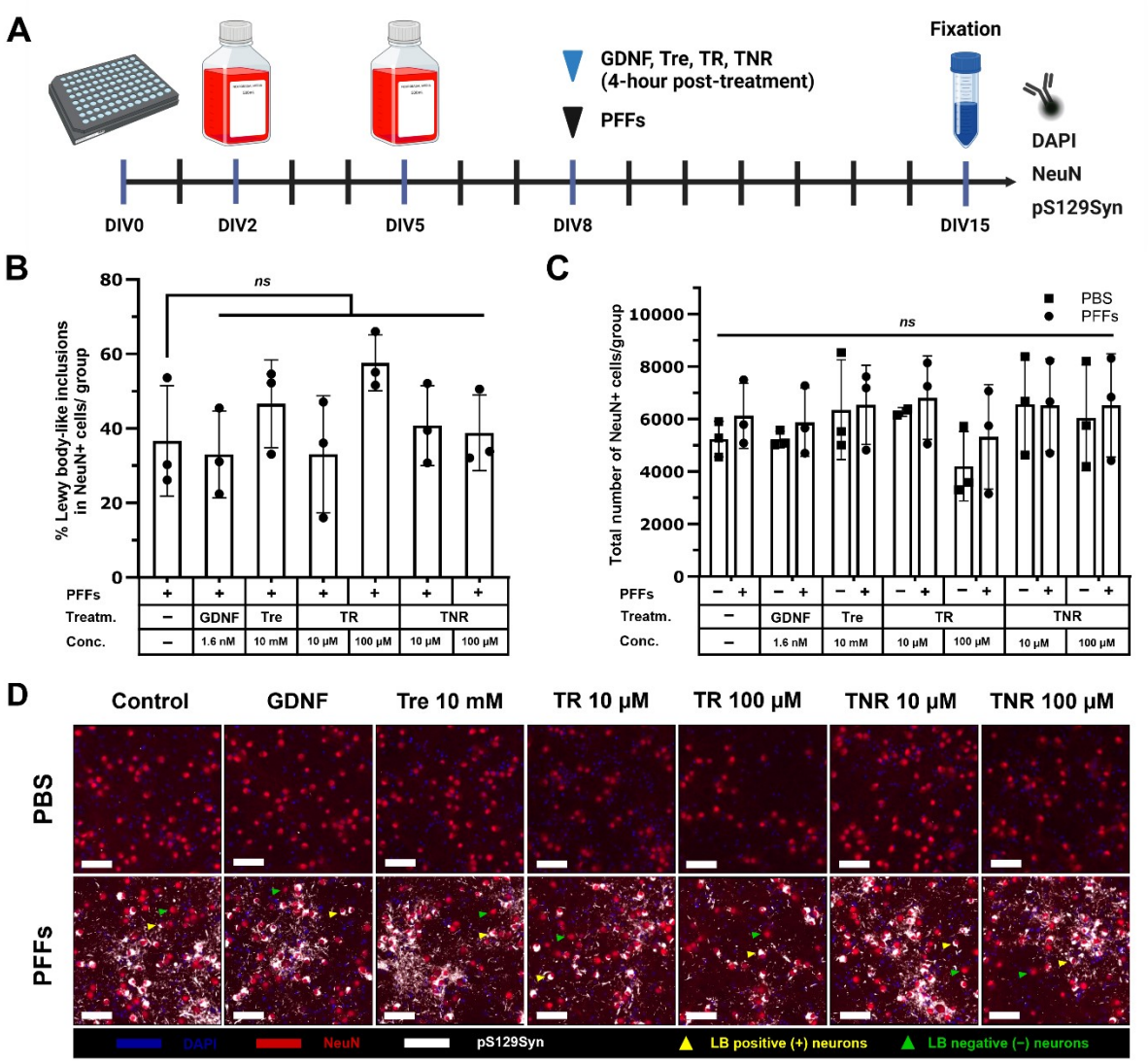

Figure S8. (A) Schematic diagram of 4-hour post-treatment timeline in hippocampal neurons, from DIV0 to DIV15. (B) Quantification of LB-like inclusions in NeuN+ cells, expressed as a percentage (%) of total NeuN+ cells in the PFFs group. (C) Quantification of the total number of NeuN+ cells per group in both PFFs and PBS groups. Data are presented as mean ± SD, from $n = 3$ independent experiments. Statistical significance: *ns* = not significant; analyzed with (B) RM One-way ANOVA with Tukey's multiple comparison test and (C) Two-way ANOVA with Šidák's multiple comparison test. (D) Representative images of different treatment groups with PBS, PFFs, and test compounds; pS129Syn immunostaining visualized LB-like inclusions in the neuron cell bodies (perinuclear, dense inclusions around NeuN) and neurites (fibrillar structures). Scale bar: 50 µm.

Quantification of LB-like inclusions in NeuN+ cells treated with PFFs and test compounds (24-hour post-treatment)

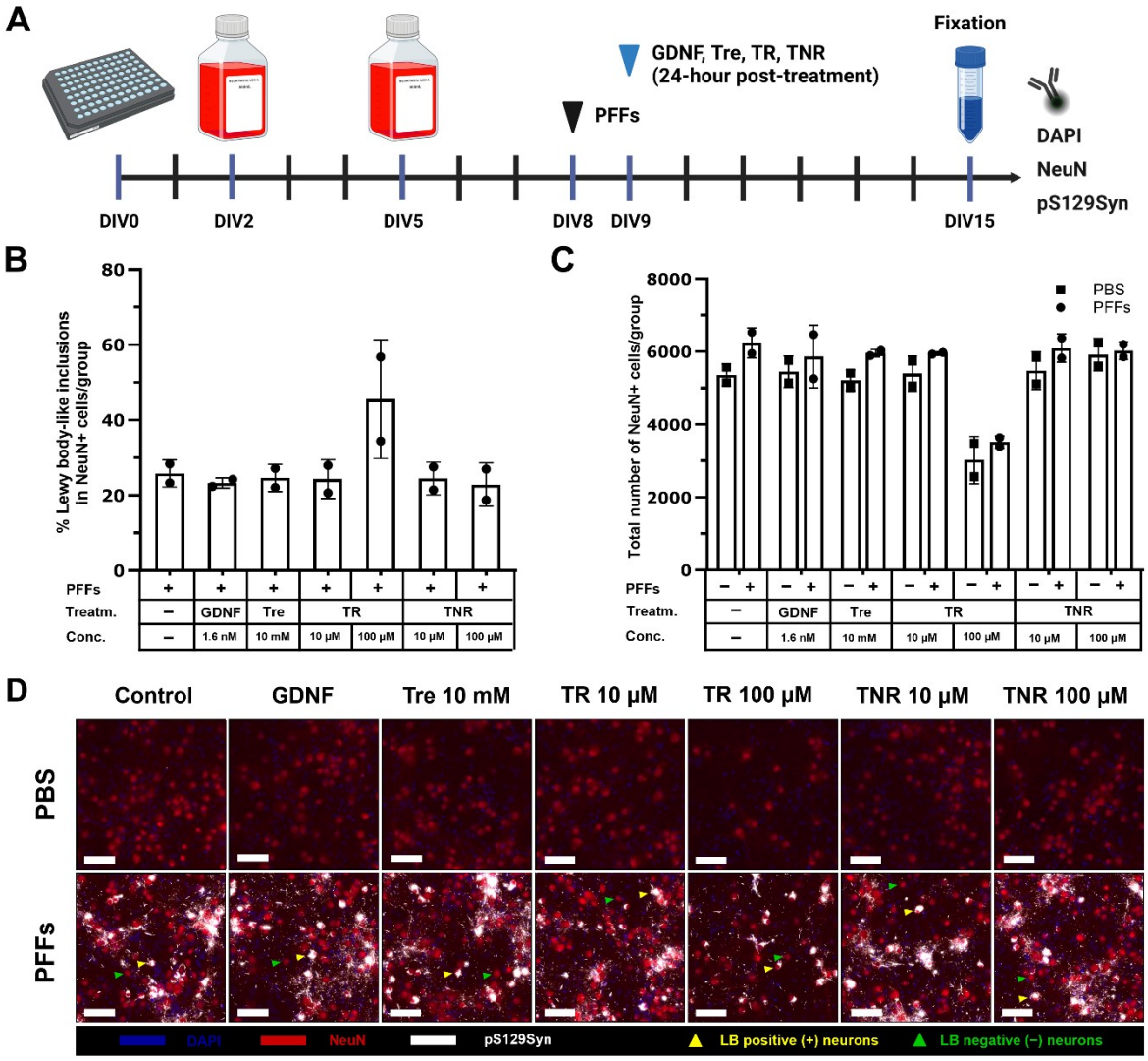

Figure S9. (A) Schematic diagram of 24-hour post-treatment timeline in hippocampal neurons, from DIV0 to DIV15. (B) Quantification of LB-like inclusions in NeuN+ cells, expressed as a percentage (%) of total NeuN+ cells in the PFFs group. (C) Quantification of the total number of NeuN+ cells per group in both PFFs and PBS groups. Data are presented as mean ± SD, from n = 2 independent experiments. (D) Representative images of different treatment groups with PBS, PFFs, and test compounds (24-h post-treatment); pS129Syn immunostaining visualized LB-like inclusions in the neuron cell bodies (perinuclear, dense inclusions around NeuN) and neurites (fibrillar structures). Scale bar: 50 µm.

Confocal images of GFP-transduced neurons treated with Cy5-labeled TR nanogel

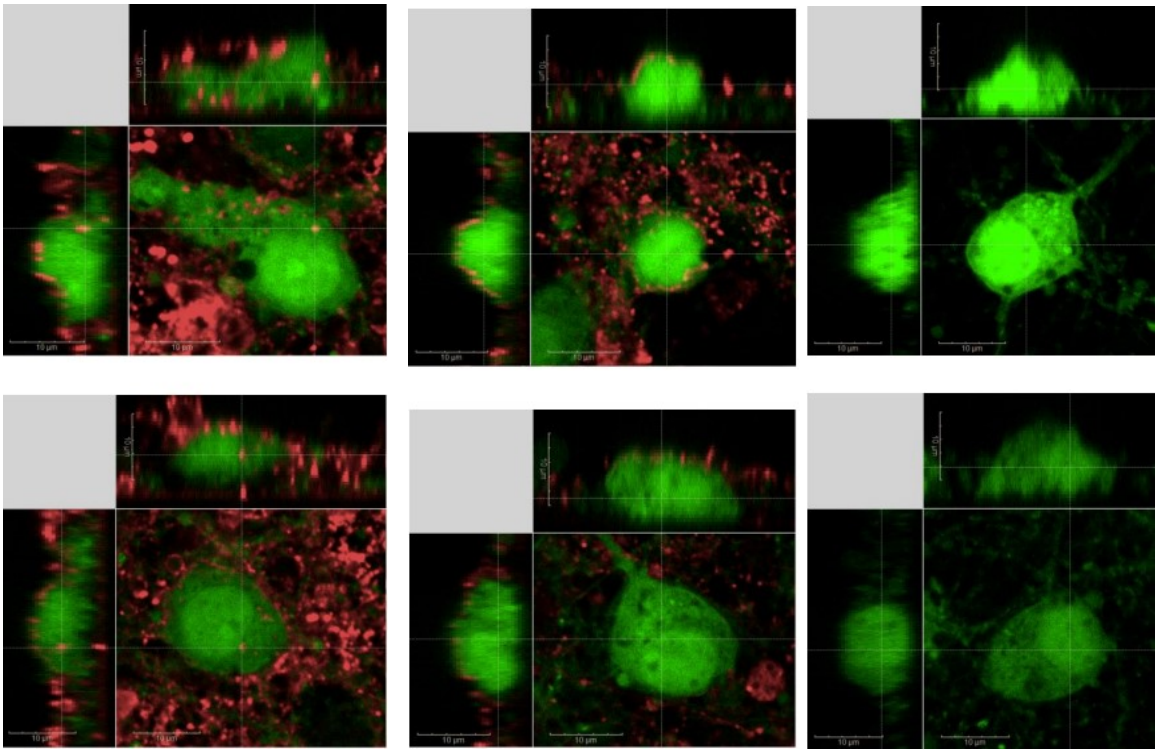

Figure S10. Confocal images of selected GFP-transduced neurons (expressing a cytoplasmic marker under the neuron specific hSyn promoter) treated with Cy5-labeled TR nanogel. Hippocampal cultures were seeded at 35k cells per well in a 96-well plate and treated with 10 mM TR nanogels at DIV13-14, followed by fixation at DIV14. The times indicated below correspond to the duration of treatment.

Colocalization of p62 and LB-like inclusions, as well as MAP2 in the PBS group (vehicle control, 1-hour pre-treatment)

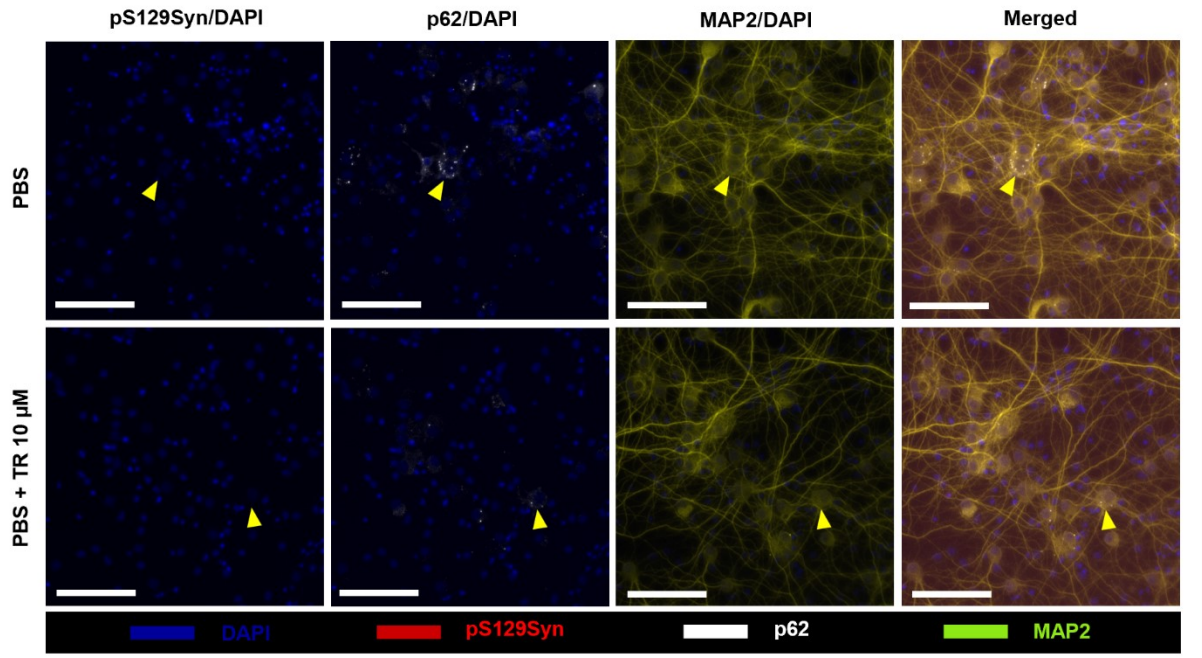

Figure S11. Representative images of colocalization of p62 and LB-like inclusions, as well as MAP2for 1-hour pre-treatment with TR 10 µM vs. (untreated) control in the PBS group (n = 3 independent experiments). Scale bar: 100 µm. Note: p62 is a key regulator in basal autophagy and is constitutively expressed in normal cells. As shown in **Figure S9** above, the p62 fluorescence signal is markedly lower than in the PFFs-treated group (**Figure 4D**), where p62 accumulates prominently due to aggregation and colocalizes well with pS129Syn aggregates.

Evaluation of autophagy induction by Tre, TR, and TNR in SH-SY5Y cells

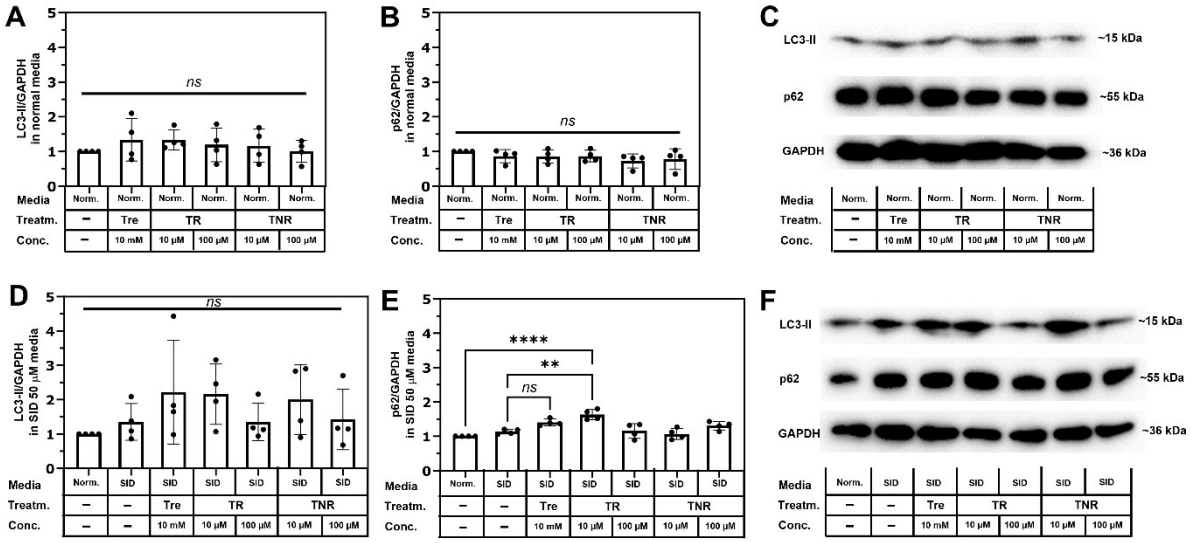

Figure S12. (A-F) Evaluation of autophagy induction by Tre, TR, and TNR in SH-SY5Y cells, using LC3-II and p62 markers, assessed by Western blot analysis. Panels (C) and (F) show representative Western blot images in normal medium and SID 50 μM medium, respectively. (A, D) Quantification of LC3-II/GAPDH ratio in (A) normal medium and (B) SID 50 μM medium. (B, E) Quantification of p62/GAPDH ratio in (B) normal medium and (E) SID 50 μM medium. Data are presented as mean ± SD, from $n = 4$ independent experiments. Statistical significance: *ns* = not significant, ** $p < 0.01$, and **** $p < 0.0001$; analyzed with RM One-way ANOVA with Tukey's multiple comparison test. Conclusion: the results suggest that TR 10 μM can induce autophagy, while free trehalose also demonstrates autophagy-inducing potential. Both Tre 10 mM and TR 10 μM exhibit a tendency to activate autophagy, as evidenced by a slight increase in LC3-II levels and a minor decrease in p62 levels in normal medium. In SID 50 μM medium, or under lysosomal blockade, TR 10 μM showed trend in increased LC3-II levels, though this was not statistically significant, while the increase in p62 levels was statistically significant, confirming TR nanogel's capability to induce autophagy. Similarly, Tre 10 mM treatment increased LC3-II and p62 levels in the SID medium; although the increase was not statistically significant, it suggests trehalose's potential to induce autophagy. Further studies are required to elucidate the precise mechanisms underlying this autophagy induction.

Colocalization of p62 and LB-like inclusions, and quantification of pSer129Syn, p62, and MAP2 levels (2-hour post-treatment)

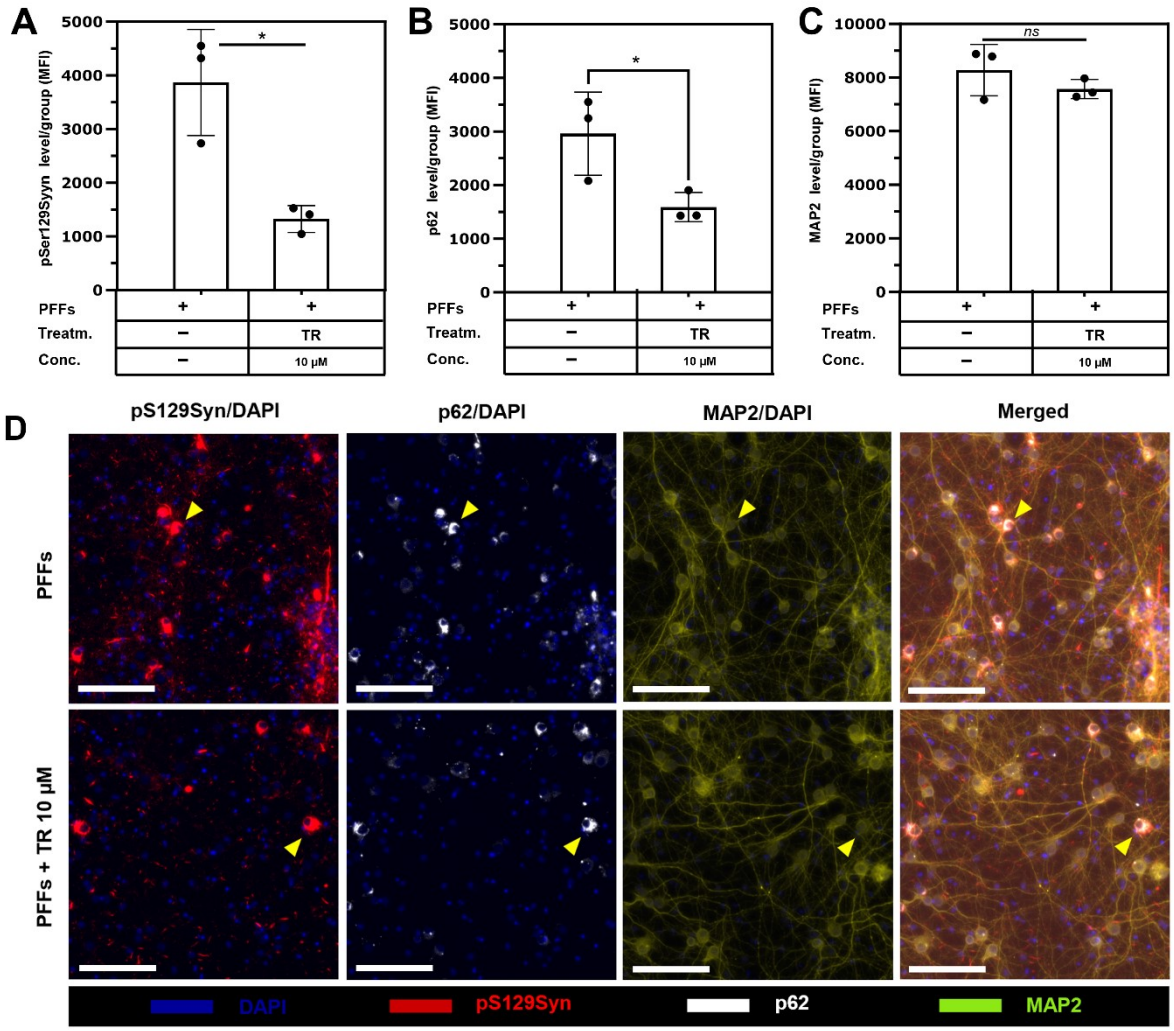

Figure S13. (A–C) Quantification of (A) pSer129Syn, (B) p62, and (C) MAP2 levels based on mean fluorescence intensity (MFI) for 2-hour post-treatment with TR 10 µM vs. (untreated) control in hippocampal neurons after 7 days in the PFFs group. Data are presented as mean ± SD, from $n = 3$ technical well repeats. Statistical significance: *ns* = not significant, * $p < 0.05$, analyzed with unpaired t-test. (D) Representative images of colocalization of p62 and LB-like inclusions for 2-hour post-treatment with TR 10 µM vs. (untreated) control. Scale bar: 100 µm.

Colocalization of p62 and LB-like inclusions, and quantification of pSer129Syn, p62, and MAP2 levels (4-hour post-treatment)

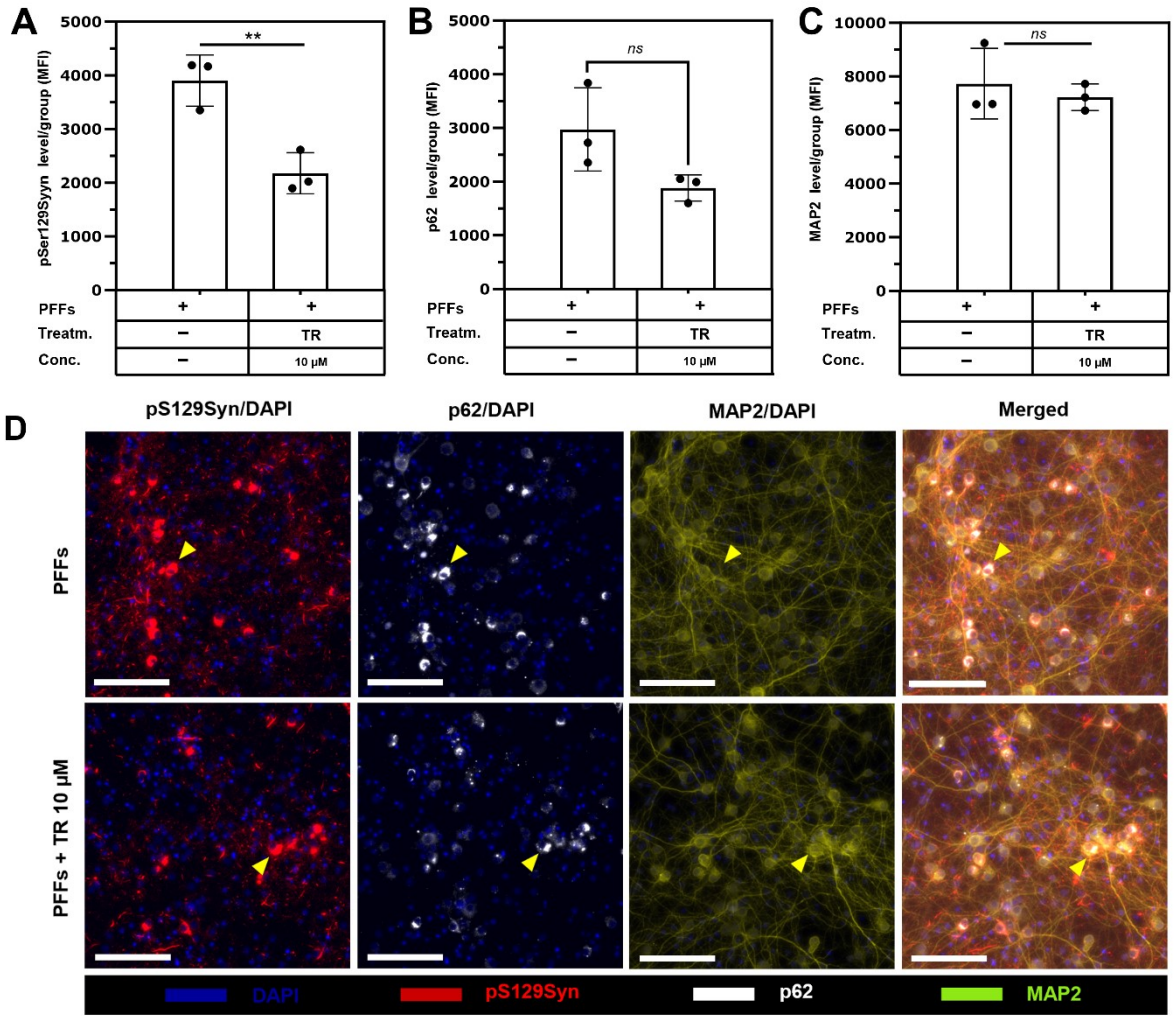

Figure S14. (A–C) Quantification of (A) pSer129Syn, (B) p62, and (C) MAP2 levels based on mean fluorescence intensity (MFI) for 4-hour post-treatment with TR 10 µM vs. (untreated) control in hippocampal neurons after 7 days in the PFFs group. Data are presented as mean ± SD, from $n = 3$ technical well repeats. Statistical significance: *ns* = not significant, * $p < 0.05$, analyzed with unpaired t-test. (D) Representative images of colocalization of p62 and LB-like inclusions for 2-hour post-treatment with TR 10 µM vs. (untreated) control. Scale bar: 100 µm.